BUTTERWORTH HEINEMANN

Polymer Vol. 36 No. 24, pp. 4665–4674, 1995

0032-3861/95/$10.00 + 0.00

Photochemistry and photoinitiator properties of 2-substituted anthraquinones: 2. Photopolymerization and flash photolysis

Norman S. Allen*, Graeme Pullen, Milla Shah and Michele Edge
Chemistry Department, Faculty of Science and Engineering, Manchester Metropolitan University, Chester Street, Manchester M1 5GD, UK

and Iain Weddell and Ron Swart
Zeneca Specialities Ltd, Blackely, Manchester M9 3DA, UK

and Fernando Catalina
Instituto de Ciencia y Tecnologia de Polymeros, CSIC, 3 Juan de la Cierva, 28006 Madrid, Spain
(Received 24 November 1994; revised 26 March 1995)

The photoinduced polymerization activities of fifteen 2-substituted anthraquinones have been determined in different monomers and prepolymers using real-time Fourier-transform infra-red spectroscopy and photocalorimetry. The relative order in photoinitiator efficiency is found to be highly dependent upon the method used, the nature of the light source, amine co-synergist and monomer being crucial factors. Oxygen quenching in all cases indicates that the triplet state is the active precursor. Without an amine co-synergist, absolute quantum-yield measurements show that anthraquinones with electron-withdrawing groups are more active than those which are electron-donating. However, in the presence of a tertiary amine and under polychromatic illumination, the effects are different. In the latter case amido derivatives with long-wavelength charge-transfer bands and mixed $n\pi^*/\pi\pi^*$ triplet states tend to be more reactive. Fluorescence and phosphorescence analyses indicate a high rate of intersystem crossing to the triplet state. The relative positions of the lowest excited singlet $\pi\pi^*$ and second excited $n\pi^*$ triplet states play an important role in determining their photoactivities, as shown in paper 1. Semiquinone radical and radical-anion intermediates are observed using microsecond flash photolysis and the data interrelated to their spectroscopic and photopolymerization activities. The haloanthraquinones are shown to undergo an additional mechanism involving dehalogenation.

(Keywords: substituted anthraquinones; photopolymerization; flash photolysis)

INTRODUCTION

In part 1[1] the photophysical properties of fifteen 2-substituted anthraquinones (structures **1** to **15**) were determined in various solvents. Absorption spectra distinguished two types of structures. The first were those with a long-wavelength band around 360 nm associated with electron-donating effects of the substituent. The second were those with a long-wavelength band around 320 nm associated with electron-withdrawing effects of the substituents. Fluorescence and phosphorescence analysis indicated a high rate of intersystem crossing to the triplet state. The relative positions of the lowest excited singlet $\pi\pi^*$ and second excited $n\pi^*$ triplet states play an important role in determining their luminescence behaviour and potential photoactivities. The electron-withdrawing and -donating ability of the 2-substituent appeared to be important in this regard. Two of the anthraquinones, 2-(4-phenyl)thiazole and 2-chloroamido, gave anomalous dual phosphorescence emissions from their triplet $\pi\pi^*$ and $n\pi^*$ states depending upon the wavelength of excitation.

Our previous work[2–4] on the photoinduced cross-linking and initiation properties of 2-substituted anthraquinone molecules showed a peculiar high degree of activity for amido groups. The 2-acrylamido-anthraquinone exhibited the highest activity. Through laser flash photolysis studies, this was associated with the importance of a long-lived active low-lying excited triplet state. In this paper we have undertaken a detailed photopolymerization study on the range of 2-substituted anthraquinones (structures **1–15**). This comparative study will enable the importance of structural features to be interrelated to their photophysical properties (paper 1)[1]. Microsecond flash photolysis studies have also been undertaken here to determine the nature of free-radical intermediates. Photoinduced polymerization studies have been undertaken in different monomers and prepolymers using real-time Fourier-transform infra-red spectroscopy and photocalorimetry. Both

* To whom correspondence should be addressed

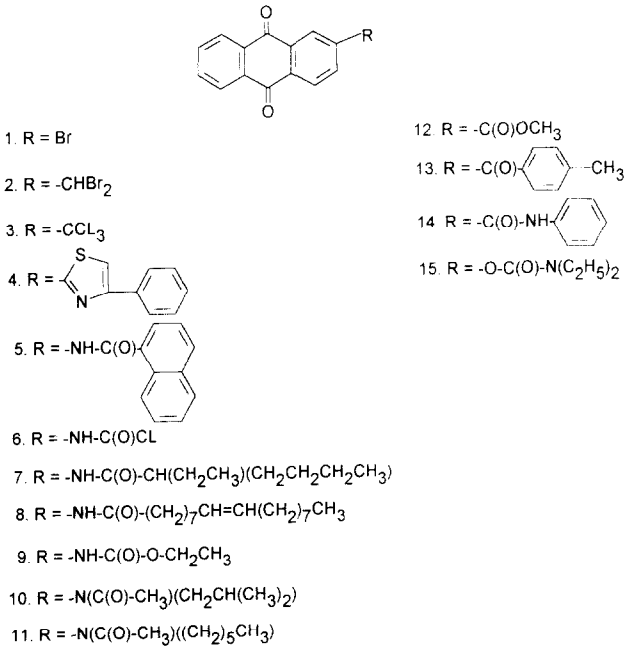

monochromatic and polychromatic irradiation conditions were employed. The data indicate that the relative efficiencies of the anthraquinones are determined not only by the methodology used but also by the nature of the light source and the presence of an amine co-synergist.

EXPERIMENTAL

Materials

The compounds, structures **1** to **15**, are named in part 1[1] and were supplied by the Fine Chemicals Service of Zeneca Specialities, Blackely, Manchester, UK. All the solvents, 2-diethylaminoethanol and triethylamine used in this work were obtained from Aldrich Chemical Co. Ltd, UK, and were of spectroscopic or h.p.l.c. grade quality.

Rates of photopolymerization

Real-time FT *i.r.* The anthraquinones (AQ) were dissolved in a minimum quantity (2–3 cm^3) of tetrahydrofuran (except AQ **4**, **6**, **7** and **11**, which were dissolved in ethanol), followed by mixing with a prepolymer based on a 50/50 (w/w) vinyl urethane/triethylene glycol dimethacrylate (VU/TGA) system (Zeneca Specialities, UK). Traces of solvent were then removed by flushing with argon for 30 min followed by addition of 1% (w/w) of the co-initiator, *p*-ethyldimethylaminobenzoate (EDB).

The resin was then placed between pieces of low-density polyethylene using a separator to give a film thickness of 50 μm. The polyethylene holder was then placed between two infra-red salt flats and placed in the sample beam. Two polyethylene film samples were used as the reference. The decrease in absorbance at 1638 cm^{-1} of the vinyl absorption band was then monitored in real-time mode during irradiation using a fibre optic arrangement. The irradiation source used here was an ILC 302UV (Laser Lines Ltd, Beaumont Close, Banbury, Oxon, UK) switchable between u.v. and visible light with a cut-off at 400 nm.

Photocalorimetry. The set-up for photocalorimetry (photo-d.s.c.) is as described previously using a modified Perkin-Elmer differential scanning calorimeter[5]. The sample and reference are irradiated by way of two fibre optic cables carrying the light energy from a high-pressure 100 W Hanovia mercury lamp and then by way of a monochromator for isolation of the 365 nm line. Heat evolution (mcal) with time of conversion is measured by maintaining the sample chamber at 40°C. The exotherm curve for each experiment is integrated to calculate the area under the curve at given time intervals. Corrections are then made for reaction times and sample weights. Lauryl acrylate was used as the monomer (Aldrich Chemical Co. Ltd, Spain) after distillation using a 20 μl sample in each case. Three experimental conditions were used, nitrogen, nitrogen and 2-diethylaminoethanol (amine) (10^{-4} M) and air and amine at $\sim 10^{-4}$ M of initiator, to give constant absorbance at 365 nm.

Plots of percentage conversion with time were obtained from which second plots of moles per litre *versus* time in seconds were obtained. From the initial slopes of the second plots, R_p values (mol l^{-1} s^{-1}) were obtained. A third plot of moles converted *versus* energy absorbed, correcting for absorption differences, was also obtained. This plot compares the efficiency of the photoinitiators in converting the light energy into polymers. The slope of this graph gives the value of the quantum yield of photopolymerization (Φ_m), i.e. the number of monomer molecules consumed per photon absorbed.

Microsecond flash photolysis

End-of-pulse transient absorption spectra on the microsecond timescale were obtained using a kinetic flash photolysis apparatus equipped with two xenon-filled flash lamps (operated at 10 kV) and a 150 W tungsten–halogen monitoring source. Transient decay

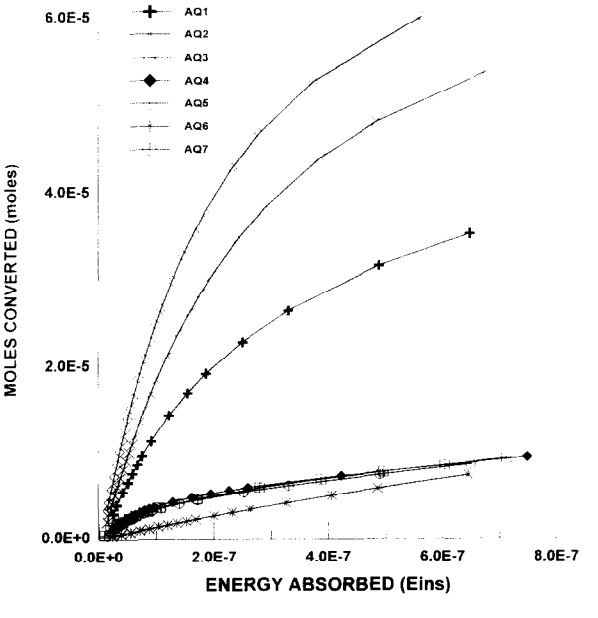

Figure 1 Conversion of anaerobic (N_2) lauryl acrylate (mol) from monomer to polymer *versus* energy absorbed (E_{ins}) for irradiation at 365 nm using photocalorimetry with 2-substituted anthraquinone photoinitiators 1–7

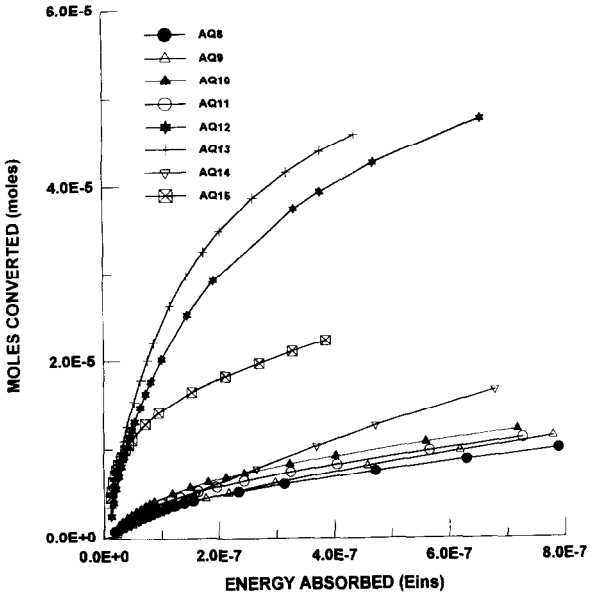

Figure 2 Conversion of anaerobic (N_2) lauryl acrylate (mol) from monomer to polymer *versus* energy absorbed (E_{ins}) for irradiation at 365 nm using photocalorimetry with 2-substituted anthraquinone photoinitiators **8–15**

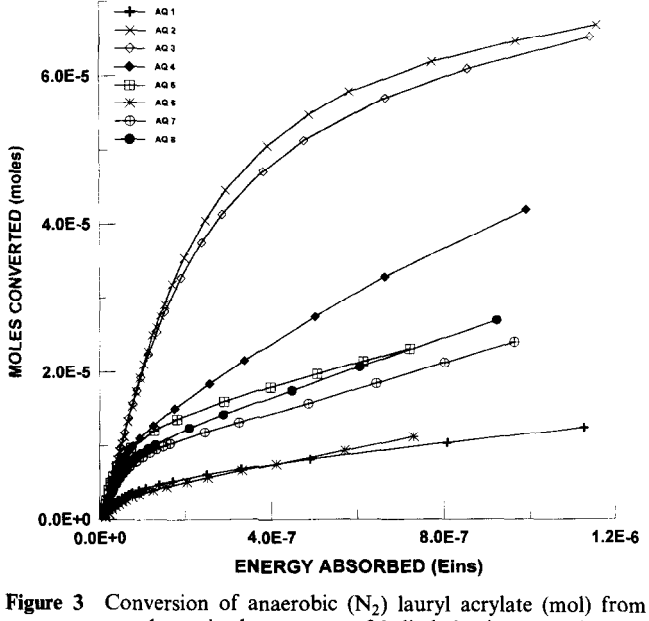

Figure 3 Conversion of anaerobic (N_2) lauryl acrylate (mol) from monomer to polymer in the presence of 2-diethylaminoethanol *versus* energy absorbed (E_{ins}) for irradiation at 365 nm using photocalorimetry with 2-substituted anthraquinone photoinitiators **1–8**

profiles were stored using a Gould model 1425 storage oscilloscope. Solutions were degassed using white-spot nitrogen gas (< 5 ppm O_2).

RESULTS AND DISCUSSION

Photopolymerization

Photocalorimetry. Using photocalorimetry three conditions were studied: (1) anaerobic, (2) anaerobic with amine and (3) aerobic with amine. Initial graphs were then obtained for the conversion of lauryl acrylate monomer ($mol\,l^{-1}$) *versus* irradiation time. Since monochromatic light was used for irradiation, corrections

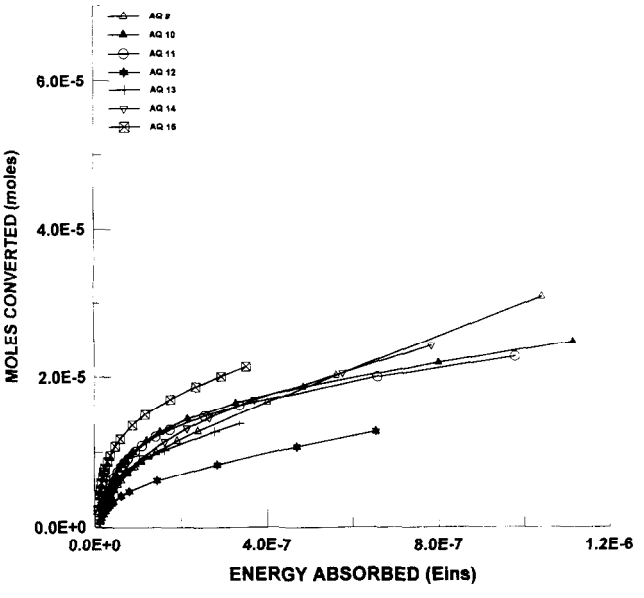

Figure 4 Conversion of anaerobic (N_2) lauryl acrylate (mol) from monomer to polymer in the presence of 2-diethylaminoethanol *versus* energy absorbed (E_{ins}) for irradiation at 365 nm using photocalorimetry with 2-substituted anthraquinone photoinitiators **9–15**

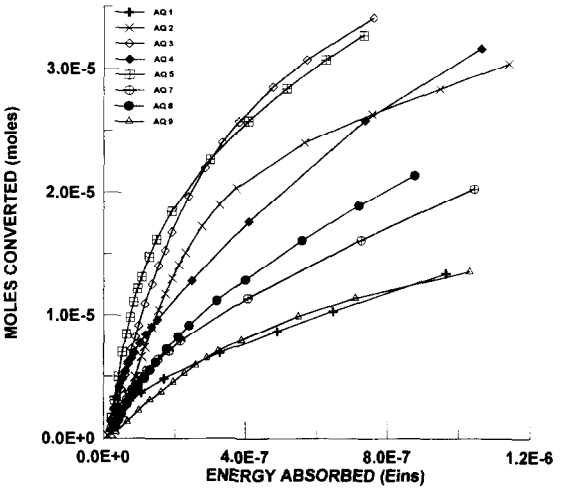

Figure 5 Conversion of aerobic lauryl acrylate (mol) from monomer to polymer in the presence of 2-diethylaminoethanol *versus* energy absorbed (E_{ins}) for irradiation at 365 nm using photocalorimetry with 2-substituted anthraquinone photoinitiators **1–9**

for the actual absorbed energy were then undertaken to present a more accurate picture of the photoactivities of the anthraquinone molecules. Conversion graphs are illustrated in *Figures 1* to *6* respectively for the three conditions used, where two graphs are used to illustrate all the anthraquinones under each condition. This allows ease of comparison for differences in rates. Comparison of the respective data shows that the order in efficiency in terms of conversion of the monomer is:

$$\mathbf{3} > \mathbf{13} > 2 > 12 > 1 > 15 > 14 > 10 > 11$$

$$> \mathbf{9} > \mathbf{8} > \mathbf{5} > \mathbf{4} > \mathbf{7} > \mathbf{6}$$

These orders in photoinitiation efficiency provide an interesting comparison in terms of our earlier spectroscopic data in part 1[1]. Compounds **1** to **3** are halogenated derivatives and have a lowest excited triplet $n\pi^*$ state. These three molecules are in the high range of

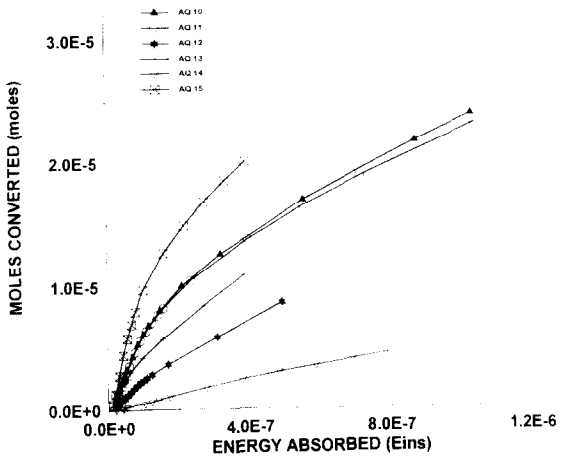

Figure 6 Conversion of aerobic lauryl acrylate (mol) from monomer to polymer in the presence of 2-diethylaminoethanol *versus* energy absorbed (E_{ins}) for irradiation at 365 nm using photocalorimetry with 2-substituted anthraquinone photoinitiators **10**–**15**

Table 1 Rates of photopolymerization (R_p) and quantum yields of photopolymerization (θ_m) of lauryl acrylate irradiated at 365 nm using 2-substituted anthraquinones as photoinitiators[a]

	Nitrogen		Nitrogen/amine		Air/amine	
Anthraquinone	R_p	θ_m	R_p	θ_m	R_p	θ_m
1	0.0194	146.1	0.0089	67.0	0.0076	56.6
2	0.0155	194.8	0.0169	228.4	0.0059	74.0
3	0.0260	322.3	0.0182	230.3	0.0089	109.9
4	0.0056	41.4	0.0210	178.8	0.0156	114.9
5	0.0048	58.5	0.0236	300.9	0.0161	165.1
6	0.0018	13.6	0.0079	59.3	–	–
7	0.0060	45.3	0.0180	136.0	0.0083	62.3
8	0.0058	44.5	0.0180	136.0	0.0069	48.9
9	0.0049	36.9	0.0186	139.2	0.0036	27.0
10	0.0075	57.3	0.0210	157.9	0.0092	71.1
11	0.0067	53.2	0.0190	143.9	0.0093	69.0
12	0.0248	321.2	0.0083	107.2	0.0021	27.0
13	0.0180	360.0	0.0100	216.1	0.0029	59.9
14	0.0031	35.9	0.0100	122.6	–	–
15	0.0160	327.7	0.0190	401.9	0.0055	114.3

[a] R_p = mol dm^{-3} s^{-1}; Amine = *N*, *N*-diethylethanolamine

Table 2 Data extrapolated from real-time *FT* i.r. analysis with u.v. and visible irradiation: with amine

	U.v. light			Visible light		
Sample AQ	Final conversion (%)	R_p (mol dm^{-3} s^{-1})	Residual unsaturation (%)	Final conversion (%)	R_p (mol dm^{-3} s^{-1})	Residual unsaturation (%)
1	42.37	2.02	57.63	22.78	1.40	77.22
2	73.63	9.49	26.37	62.21	4.94	37.79
3	68.77	7.02	31.23	59.61	4.34	40.39
4	61.06	4.07	38.94	62.78	3.71	37.22
5	66.01	8.10	33.99	67.35	8.63	32.65
6	42.80	2.23	57.20	46.50	2.23	53.50
7	70.25	7.90	29.75	66.14	8.38	33.86
8	73.25	6.67	26.75	70.35	6.15	29.65
9	61.58	4.96	38.42	60.86	4.91	39.14
10	63.45	5.29	36.55	61.25	4.48	38.75
11	62.07	5.33	37.93	59.86	4.12	40.14
12	56.19	3.70	43.81	30.58	1.77	69.42
13	58.30	3.79	41.70	30.27	1.63	69.73
14	56.94	3.98	43.06	44.34	2.28	55.66
15	65.89	6.69	34.11	55.71	4.38	44.29

photoinitiation activity. Compounds **10** to **15** also possess a low-lying triplet $n\pi^*$ state, but there is evidence of some $\pi\pi^*$ character, and all appear to exhibit medium to high photoinitiation activity. However, both these categories exhibit a longest-wavelength absorption maximum at around 320–330 nm in the near-u.v. that is characteristic of a $n\pi^*$ transition. The other molecules **4** and **6** exhibit a strongly mixed triplet $n\pi^*/\pi\pi^*$ state, while molecules **5**, **7**, **8** and **9** exhibit a low-lying triplet $\pi\pi^*$ state. All the molecules **4** to **9** exhibit long-wavelength absorption maxima above 360 nm indicative of a strong charge-transfer (CT) content and all exhibit low photoinitiation activity.

The most interesting feature of the photo-d.s.c. data is that all the anthraquinones **5** to **9**, with an electron-donating group, have low photoinitiation activity, whilst the compounds **1** to **3** and **10** to **15**, which have an electron-withdrawing group, exhibit higher activities. For absolute photochemistry the photo-d.s.c. data are more quantitative and realistically valid for comparative purposes with the photophysical properties of the initiators. This is because differences in the absorption energies of the molecules have been corrected. From an industrial point of view, however, such comparisons would be unreal since polychromatic irradiation sources are used and therefore the total energy absorbed over a much broader range of wavelengths has to be taken into consideration as well as the energies and configurations of their excited triplet states. Another aspect is the viscosity of the monomer/prepolymer used. This will be illustrated further with the real-time *FT* i.r. data.

From the data in *Figures 1* to *6* the early initial rates of photopolymerization are also important. These exhibit very different trends from those of the overall rates. From the linear portion of these curves, quantum yields of photopolymerization may be calculated and the data

Table 3 Data extrapolated from real-time *FT* i.r. analysis with u.v. and visible irradiation: without amine

	U.v. light			Visible light		
Sample AQ	Final conversion (%)	R_p (mol dm^{-3} s^{-1})	Residual unsaturation (%)	Final conversion (%)	R_p (mol dm^{-3} s^{-1})	Residual unsaturation (%)
1	40.51	2.56	59.49	14.37	0.98	85.63
2	68.36	7.65	31.64	39.92	2.98	60.08
3	63.40	7.90	36.60	58.41	4.15	41.59
4	11.64	0.64	88.36	14.24	0.63	85.76
5	41.93	2.56	58.07	38.47	1.87	61.53
6	3.47	0.45	96.53	4.71	0.19	95.29
7	46.91	2.79	53.09	35.67	1.68	64.33
8	42.88	2.06	57.12	43.10	2.04	56.90
9	29.09	1.75	70.19	20.25	1.11	79.75
10	37.19	1.26	62.81	17.70	1.00	82.30
11	44.45	2.40	55.55	22.20	1.15	77.80
12	56.37	4.14	43.63	25.84	1.36	74.16
13	56.72	4.12	43.28	25.99	1.45	74.01
14	34.17	1.58	65.83	6.33	0.31	93.67
15	60.84	6.43	39.16	8.19	0.43	91.81

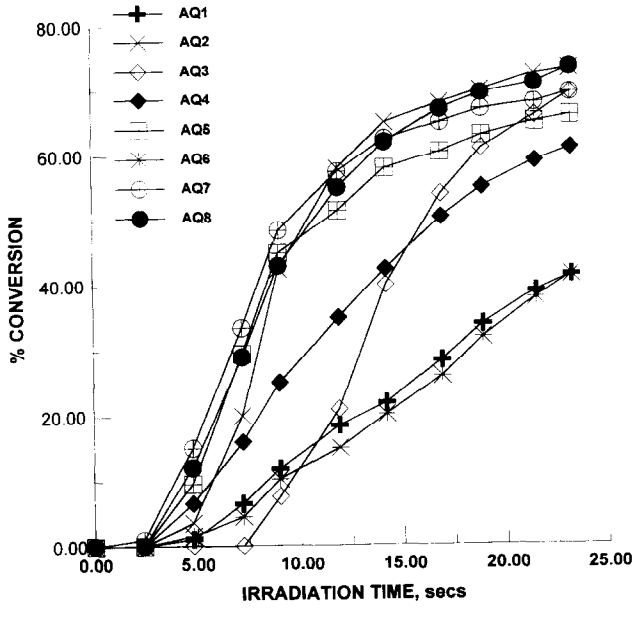

Figure 7 Percentage conversion *versus* time of irradiation with u.v. light (< 400 nm) of a VU/TGA prepolymer containing 0.001 mol% of 2-substituted anthraquinones **1**–**8** with 1% (w/w) EDB using real-time *FT* i.r.

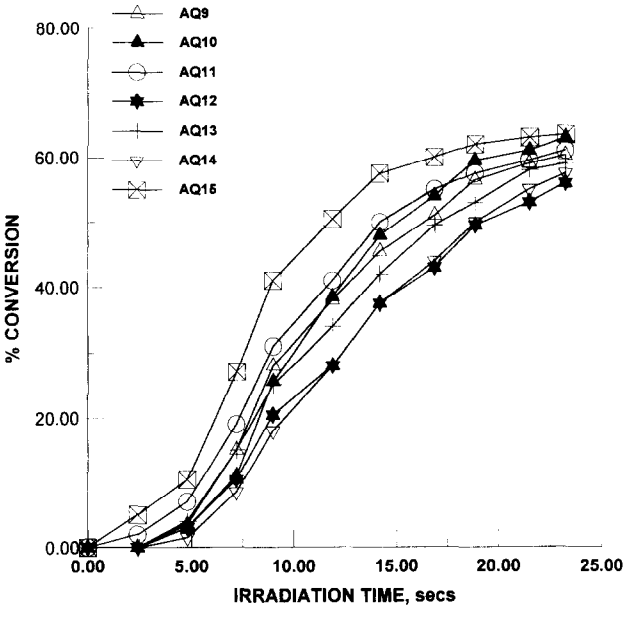

Figure 8 Percentage conversion *versus* time of irradiation with u.v. light (< 400 nm) of a VU/TGA prepolymer containing 0.001 mol% of 2-substituted anthraquinones **9**–**15** with 1% (w/w) EDB using real-time *FT* i.r.

compared for the different conditions used. The results in *Table 1* show the data for nitrogen, nitrogen/amine and air/amine conditions. From the data two features are seen. The first feature showed that, apart from the compounds **1**, **3**, **12** and **13**, the presence of a tertiary amine co-synergist accentuates the rate of photopolymerization. This effect is normally associated with the formation of an exciplex causing either electron or hydrogen-atom abstraction by the excited triplet state of the anthraquinone[6]. The absence of any synergism with the four anomalous initiators suggests that triplet quenching by the amine may be operative. In the presence of air and amine the photoactivities of all the initiators are markedly reduced, indicating the importance of the triplet state as the active precursor. The most notable feature of all the data, however, is the high activity of the two halo initiators **2** and **3**, with **6** (chloroamido) being the least active. Recent work on halo-substituted thioxanthones has shown the formation of halo radicals on irradiation[7]. Thus, for 1-chloro-4-n-propoxythioxanthone this was confirmed by the observance of amino hydrochloride formation on irradiation of cyclohexane solutions of the initiator in the presence of a tertiary amine. This experiment was repeated in this study for the three halo derivatives **1** to **3** using *N*,*N*-diethylethanolamine. In all three cases precipitate formation was observed due to the amine hydrochloride. Thus, apart from photoreduction due to the quinone

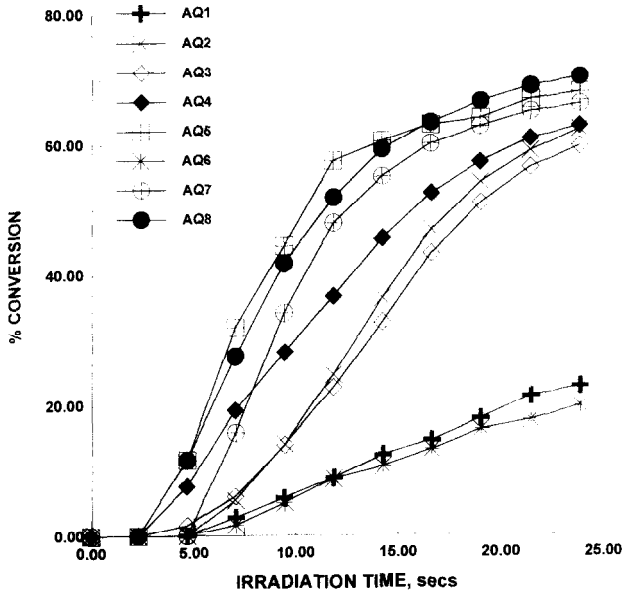

Figure 9 Percentage conversion *versus* time of irradiation with visible light (> 400 nm) of a VU/TGA prepolymer containing 0.001 mol% of 2-substituted anthraquinones **1**–**8** with 1% (w/w) EDB using real-time *FT* i.r.

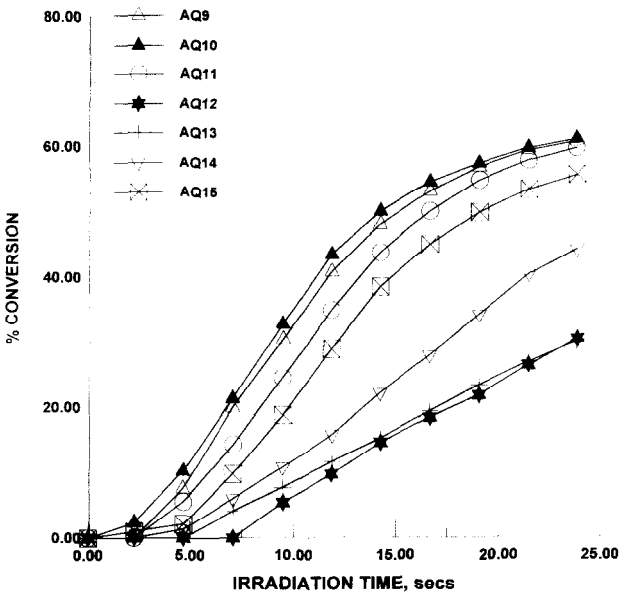

Figure 10 Percentage conversion *versus* time of irradiation with visible light (> 400 nm) of a VU/TGA prepolymer containing 0.001 mol% of 2-substituted anthraquinones **9**–**15** with 1% (w/w) EDB using real-time *FT* i.r.

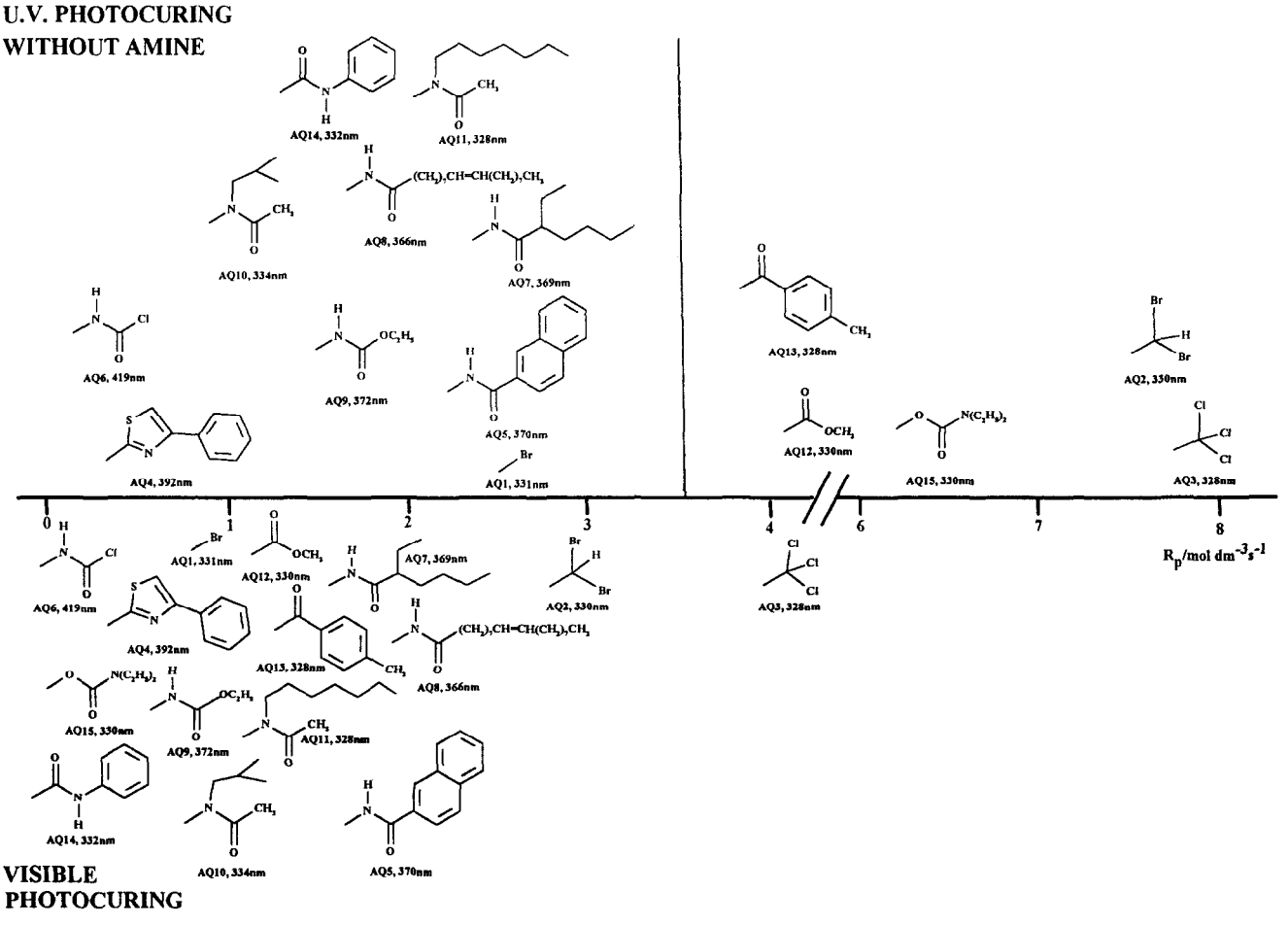

Figure 11 Correlation chart of photoinitiator structure *versus* rate of photopolymerization (mol dm^{-3} s^{-1}) from percentage conversions of VU/TGA prepolymer with u.v. and visible light, without EDB

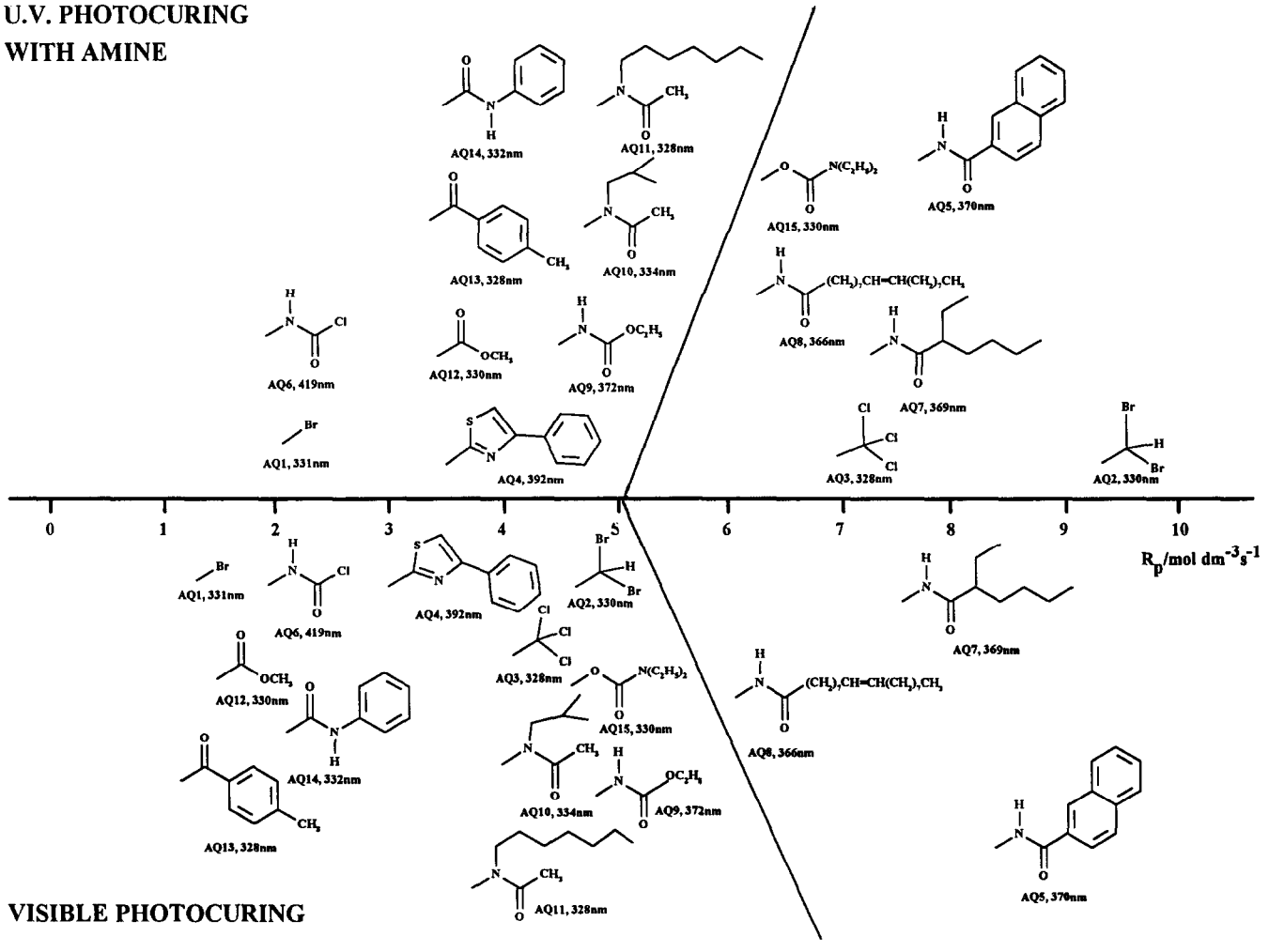

Figure 12 Correlation chart of photoinitiator structure *versus* rate of photopolymerization (mol dm^{-3} s^{-1}) from percentage conversions of VU/TGA prepolymer with u.v. and visible light, with EDB

groups, dehalogenation with the subsequent formation of active halo radicals also appears to be involved in their photoinitiation reactions and may account, in part, for their high activities.

Real-time FT *i.r.* The real-time *FT* i.r. analysis was undertaken using a viscous VU/TGA prepolymer using a polychromatic light source with a filter allowing u.v. excitation with light wavelengths less than 400 nm and visible excitation with light wavelengths above 400 nm. Both conditions were examined for all the photoinitiators in the absence and presence of a solid tertiary amine (EDB). It should be noted that in an industrial situation the presence of an amine co-synergist is considered to be an essential part of the formulation. *Tables 2* and *3* compare the sets of data obtained for u.v. and visible light exposures with and without an amine present. Each set of data provides information on the final percentage conversion, percentage residual unsaturation and the rate of propagation, R_p (mol dm^{-3} s^{-1}). The latter is again obtained from the initial linear portion of the rate curve. Actual rate curves in the presence of an amine (EDB) are illustrated in *Figures 7* and *8* for u.v. and *Figures 9* and *10* for visible light curing respectively. As can be seen, the initial and final rates are quite different for each of the photoinitiators. Thus, AQ **3** in *Figure 7* and AQ **7** in *Figure 9* exhibit induction periods before any cure and thereafter rise rapidly to a high conversion. It is to be noted that total conversion in terms of loss of unsaturation is not obtained with any of the initiators. This effect is quite common and associated with increased viscosity of the system during cure, preventing radical migration and hence polymerization.

For ease of comparison of the rates of curing, structural charts have been constructed relating the efficiencies of the different photoinitiators. Note that actual values are obtainable from the respective tables for R_p. These charts interpret the effects more clearly from a visual point of view. These data show a number of interesting features not apparent using the technique of photo-d.s.c. Without an amine co-synergist and under visible light irradiation (*Figure 11*), all the initiators exhibit very low activity. However, it is interesting to note that some degree of conversion does occur. This is noted for the trichloromethyl derivative (AQ **3**). It should be noted that, although many of the derivatives have longest-wavelength absorption maxima around 330 nm, they nevertheless exhibit some colour, i.e. they are yellow to brown crystalline powders. Consequently, they will possess a long weakly absorbing tail extending into the visible region of the spectrum but with low activity. Irradiation with u.v. light below 400 nm produces an enhanced effect on the cure rates with a somewhat better dispersal in the order. In this case it is interesting to note that all the initiators with long-wavelength $n\pi^*$ transitions exhibit the highest

photoinitiation rate, an effect consistent with the photo-d.s.c. data in the absence of an amine. The exceptions were AQ **1**, **10** and **11**. The latter two molecules exhibit some degree of mixed character with a weak CT state, e.g. in less polar solvents AQ **11** has a long-wavelength band at 360 nm. Both molecules are, in fact, weakly coloured and will exhibit a long CT tail at high concentrations. The high activities of both the halomethyl derivatives are, as shown above, due to the predominance of chorine and bromine radical formation. In the case of AQ **1** bromine directly attached to the ring system may be less susceptible to photolysis. Again, it is interesting to note that AQ **6** is the least active of the initiators.

In the presence of an amine co-synergist (*Figure 12*) the photoinitiation effects are more marked. Again, as found for the photo-d.s.c. analysis, AQ **1**, **3**, **12** and **13** did not exhibit enhanced activity in the presence of an amine co-synergist. Under visible irrradiation only the initiators with long-wavelength $\pi\pi^*$ transitions exhibited the highest activity. A line is drawn on the chart to separate them. Compound AQ **9** is only just on the left of the marker but still exhibits a similar high activity. These initiators exhibit lowest triplet $n\pi^*/\pi\pi^*$ states and strong exciplex formation with the amine. Under u.v. irradiation, photoinitiation rates are generally greater, with AQ **5**, **7** and **8** exhibiting a high activity. Again, both the halomethyl derivatives, **2** and **3**, exhibit high u.v. activity as does AQ **15**. The lower activities of compounds **4** and **6** may be due to the fact that their lowest excited triplet $n\pi^*$ and $\pi\pi^*$ states have a larger energy gap than those of

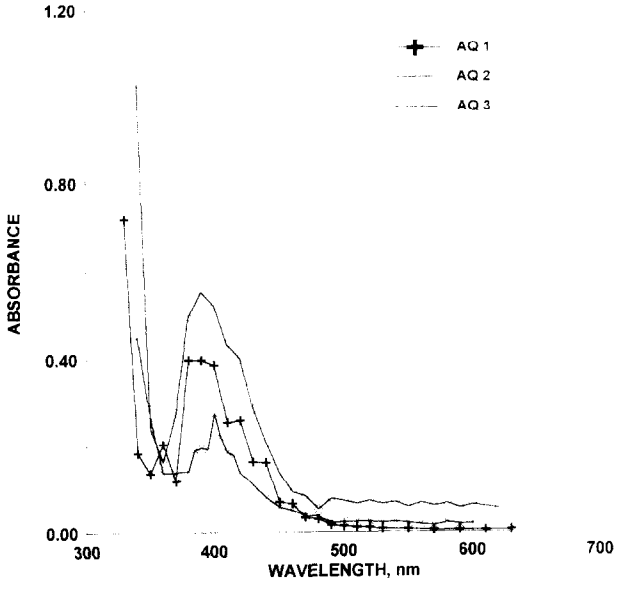

Figure 13 End-of-pulse transient absorption spectra produced on microsecond flash photolysis of 2-substituted anthraquinones **1**–**3** in anaerobic 2-propanol (10^{-5} M)

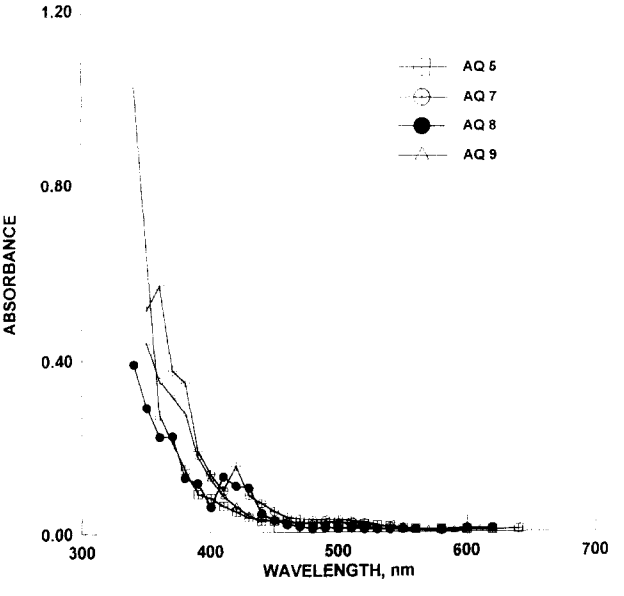

Figure 15 End-of-pulse transient absorption spectra produced on microsecond flash photolysis of 2-substituted anthraquinones **5** and **7**–**9** in anaerobic 2-propanol (10^{-5} M)

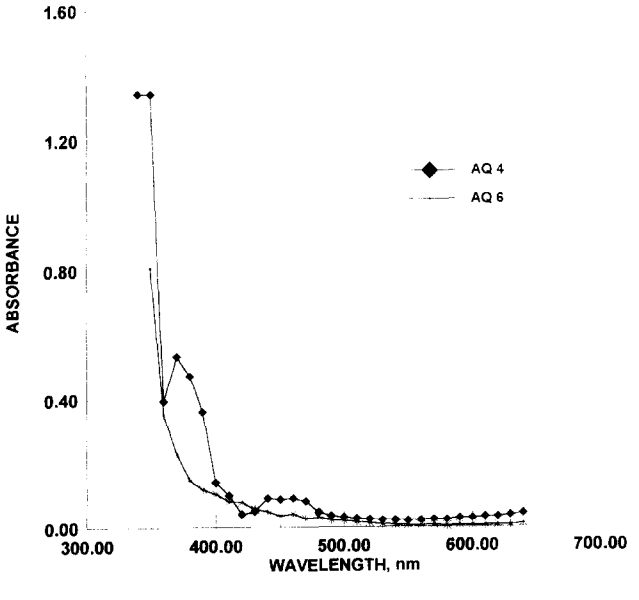

Figure 14 End-of-pulse transient absorption spectra produced on microsecond flash photolysis of 2-substituted anthraquinones **4** and **6** in anaerobic 2-propanol (10^{-5} M)

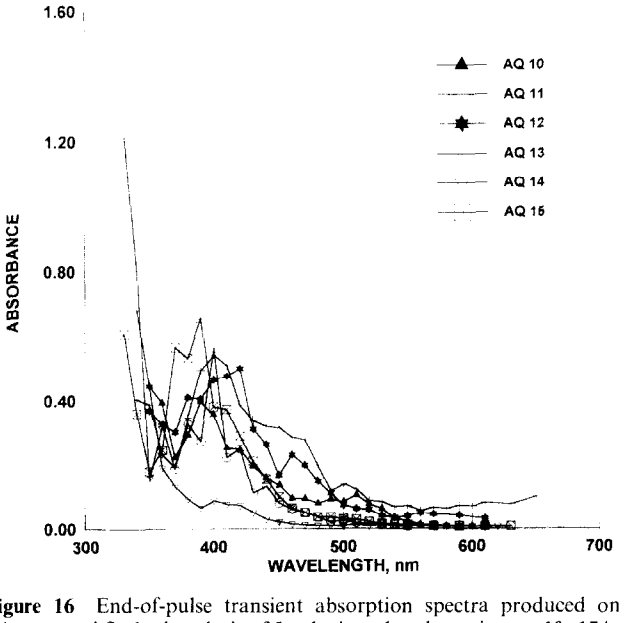

Figure 16 End-of-pulse transient absorption spectra produced on microsecond flash photolysis of 2-substituted anthraquinones **10**–**15** in anaerobic 2-propanol (10^{-5} M)

5 and **7–9**. Thus, the activity of the $\pi\pi^*$ state is expected to be lower.

Flash photolysis

End-of-pulse transient absorption spectra produced on microsecond flash photolysis are shown in *Figures 13* to *16* for derivaties 1–3, 4 and 6, 5 and 7–9, and 10–15 respectively. The first set of spectra in *Figure 13* for compounds **1** to **3** exhibit a definite maximum around 400 nm with a broad tail extending to 550–600 nm. As with all the anthraquinone spectra, there is also a sharp intense cut-off below 350 nm due to higher-energy transitions. Absorption bands in the region 350–450 nm are normally assigned to the semiquinone radical (AH·) produced by the triplet excited state of the anthraquinone (A*) abstracting a hydrogen atom from the solvent (RH) by:

$$A^* + RH \longrightarrow AH^{\cdot} + R^{\cdot} \quad (1)$$

Transient absorption spectra in the region 450–600 nm are normally weak in neutral alcohols such as 2-propanol but are considerably enhanced in basic media[8,9]. They are normally associated with the radical-anion species formed by electron transfer from a hydroxide or alkoxide species to the excited triplet state of the anthraquinone:

$$A^* + OH^- \longrightarrow A^{-\cdot} + OH^{\cdot} \quad (2)$$

The radical-anion may also be formed from the semiquinone radical and a hydroxyl anion by:

$$AH^{\cdot} + OH^- \longrightarrow A^{-\cdot} + H_2O \quad (3)$$

to give water.

Both the semiquinone radical and the radical-anion have also been shown to exist in equilibrium with each other by:

$$AH^{\cdot} \rightleftharpoons A^{-\cdot} + H^+ \quad (4)$$

Derivatives **4** and **6** in *Figure 14* give weak ill-defined spectra with no characteristic maxima for semiquinone radical apart from AQ **4**, which has a shoulder at 370 nm and a small band at 450 nm. Derivatives **5** and **7–9** are similar, with no definite absorption maxima for the semiquinone radical or radical-anion (*Figure 15*). Derivatives **7** and **8** have small bands at 420 and 410 nm, respectively, due to weak semiquinone radical formation. Compounds **10–15** in *Figure 16* all exhibit well defined spectra due to the semiquinone radical. Compounds **10**, **12** and **13** also exhibit well defined, relatively stronger absorbances due to the radical-anion. The exception is compound **14**, which exhibits only a weak band at 400 nm. All the maxima are tabulated in *Table 4* for ease of comparison.

It is interesting to note that all the compounds with high photopolymerization activity, i.e. **1–3** and **10–15**, exhibit relatively strong and well defined transient absorptions due to the semiquinone radical. This result is also consistent with the triplet $n\pi^*$ activities of the molecules, indicating that they primarily operate via a mechanism of hydrogen-atom abstraction. It is interesting to note that compounds **2**, **3**, **12** and **13** also exhibit well defined transient absorptions due to the radical-anion and are the most active of the photoinitiators, indicating strong equilibrium with the radical-anion due to electron transfer. Compound **14** has the lowest photoinitiation activity of the group and the weakest transient absorption.

The remaining compounds, **4** to **9**, all exhibit weak or ill-defined spectra, consistent with their lower photoinitiation activities and less active triplet $\pi\pi^*$ states. Direct comparisons are obviously difficult due to differences in solvent viscosities, radical mobilities and triplet quenching rates.

One final feature of the photopolymerization results is the observation that, for both photo-d.s.c. and real-time *FT* i.r. methods, the activities of the initiators **1**, **3**, **12** and **13** were not enhanced by the presence of a tertiary amine co-synergist. In order to ascertain the nature of the mechanism, a microsecond flash photolysis study was undertaken on one of these compounds (AQ **12**) together with that of AQ **11** in the absence and presence of a

Table 4 Microsecond flash transient absorption spectra of 2-substituted anthraquinone derivatives in 2-propanol (10^{-6} M)

	Transient maxima			
	Semiquinone radical		Radical-anion	
Anthraquinone	λ_{max} (nm)	Absorbance	λ_{max} (nm)	Absorbance
1	400	0.40	460	0.06
2	405	0.28	460 (s), 520	0.06, 0.02
3	395	0.57	470 (s), 490	0.10, 0.09
4	370 (s)	0.56	450	0.09
5	400 (s)	0.09	450	0.02
6	420	0.09	460	0.03
7	420	0.16	500	0.03
8	410	0.14	490	0.01
9	375 (s)	0.30	460	0.03
10	400	0.40	510	0.11
11	400	0.59	500	0.02
12	410	0.50	450 (s), 560	0.25, 0.05
13	400	0.55	450 (s), 500	0.32, 0.14
14	400	0.08	550	0.01
15	390	0.66	490 (s)	0.02

(s) = shoulder

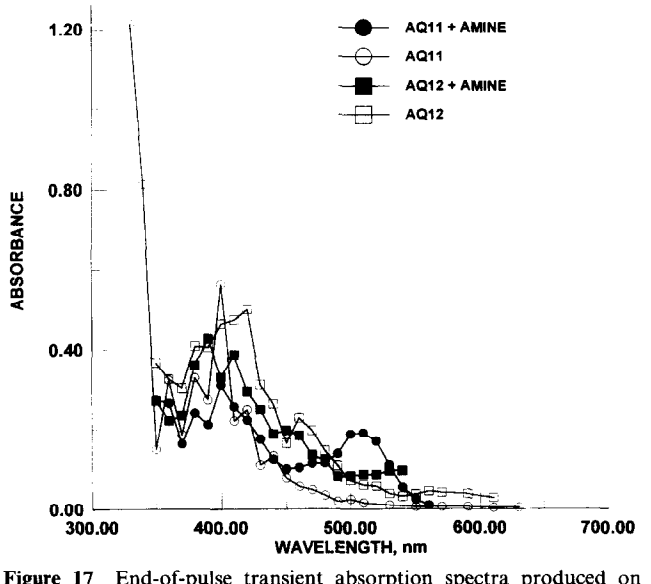

Figure 17 End-of-pulse transient absorption spectra produced on microsecond flash photolysis of 2-substituted anthraquinones (10^{-5} M) **11** and **12** with (●, ■) and without (○, □) triethylamine (10^{-4} M) respectively in anaerobic 2-propanol

tertiary amine (10^{-4} M), triethylamine. The photoactivity of the latter was found to be enhanced by the presence of a tertiary amine. End-of-pulse transient absorption spectra for these initiators are shown in *Figure 17*. For AQ **11** it is seen that, while the presence of the amine reduces the formation of the semiquinone radical at 400 nm, a new absorption appears at 510 nm associated with the formation of the radical-anion species. However, while the presence of the amine also reduces the intensity of the semiquinone radical formed with AQ **12**, no significant formation of the radical anion is observed. Thus, the enhanced effect of a tertiary amine is evidently due to the ability of the anthraquinone to abstract an electron from the amine via an intermediate exciplex. The deactivation effect of the amine in the case of AQ **12** is evidently due to triplet quenching and a consequent reduction in the degree of hydrogen-atom abstraction to form the semiquinone radical species.

CONCLUSIONS

From the results the relative order in photoinitiator efficiency is found to be highly dependent upon the method used, nature of the light source, amine co-synergist and monomer. Oxygen quenching in all cases indicates that the triplet state is the active precursor. Without an amine co-synergist, absolute quantum-yield measurements via photo-d.s.c. show that anthraquinones with electron-withdrawing groups are more active than those which are electron-donating. However, in the presence of a tertiary amine and under polychromatic illumination, the effects are different. In the latter case amido derivatives with long-wavelength charge-transfer bands and mixed $n\pi^*/\pi\pi^*$ triplet states tend to be more reactive. The ability of the photoinitiator to form an intermediate semiquinone radical via hydrogen-atom abstraction appears to be an important primary mechanism, with electron transfer being more important in the presence of an amine co-synergist. The haloanthraquinones appear to undergo an additional mechanism involving dehalogenation. The bromine and chlorine radicals may then participate in the overall initiation mechanism.

ACKNOWLEDGEMENTS

The authors would like to thank Zeneca Specialities for facilities in carrying out this work and EPSRC for a grant in supporting one of them (GP). The authors also thank NATO, Brussels, for a travel grant No. CRG/940713 in support of this programme of work.

REFERENCES

1 Allen, N. S., Pullen, G., Shah, M., Edge, M., Holdsworth, D., Weddell, I., Swart, R. and Catalina, F. *J. Photochem. Photobiol., (A) Chem. Edn.* in press
2 Allen, N. S., Hurley, J. P., Bannister, D. and Follows, G. W. *Eur. Polym. J.* 1992, **28**, 1309
3 Allen, N. S., Hurley, J. P., Bannister, D., Follows, G. W., Navaratnam, S. and Parsons, B. J. *J Photochem. Photobiol., Chem. Edn.* 1992, **68**, 213
4 Allen, N. S., Hurley, J. P., Rahman, A., Follows, G. W. and Weddell, I. *Eur. Polym. J.* 1993, **29**, 1155
5 Allen, N. S., Catalina, F., Peinado, C., Sastre, R., Mateo, J. L. and Green, P. N. *Eur. Polym. J.* 1987, **23**, 985
6 Allen, N. S. *Trends Polym. Sci.* 1993, **1**, 213
7 Allen, N. S. Mallon, D., Timms, A., Green, A. W., Catalina, F., Corrales, T., Navaratnam, S. and Parsons, B. J. *J. Chem. Soc., Faraday Trans.* 1994, **90**, 83
8 Allen, N. S. and McKellar, J. F. in 'Developments in Polymer Photochemistry–1' (Ed. N. S. Allen), Applied Science, London, 1980, Ch. 7, p. 191
9 Allen, N. S. and McKellar, J. F. 'Photochemistry of Dyed and Pigmented Polymers', Applied Science, London, 1980